Hindawi Publishing Corporation
Shock and Vibration
Volume 2015, Article ID 451583, 11 pages
http://dx.doi.org/10.1155/2015/451583

Research Article

An Improved Shock Factor to Evaluate the Shock Environment of Small-Sized Structures Subjected to Underwater Explosion

Wenzheng Zhang and Weikang Jiang

State Key Laboratory of Mechanical System and Vibration, Shanghai Jiao Tong University, Shanghai 200240, China

Correspondence should be addressed to Weikang Jiang; wkjiang@sjtu.edu.cn

Received 9 October 2014; Revised 30 March 2015; Accepted 31 March 2015

Academic Editor: Wen Long Li

Shock factor is conventionally used to assess the effect of an underwater explosion on a target. The dimensions of some structures are much smaller than the wavelength of incident wave induced by the underwater explosion. The conventional shock factor may be excessively severe for small-sized structures because it neglects the effect of scattering; so it is necessary to study the shock factor for small objects. The coupled mode method is applied to study the scattering field surrounding the cylindrical shells. A nonlinear relation differential is derived from the impact received by the cylindrical shells and the ratio between the diameters of the shells and the wavelength of the incident wave. An improved shock factor is developed based on the fitted curve, considering the scattering effect caused by the diameters of the submerged cylindrical shells. A set of numerical simulations are carried out to validate the accuracy of the proposed approach. The results show that the cylindrical shells and spherical shells under different conditions, but with the same shock factor, have almost the same shock responses.

1. Introduction

The dynamic responses and shock damage of the vessels subjected to underwater explosion (UNDEX) are important concerns for naval researchers. Cylindrical shells and spherical shells account for a large proportion in the vessels and offshore structures, especially in surface ships and submarines. Therefore, the researches on the dynamic responses and shock environment of the cylindrical shells subjected to underwater shock load make great significance in assessing the impact resistance ability of submerged structures.

Full scale test is the most direct and effective method to study how the vessels dynamically respond to and are damaged by the underwater shock wave. However, conducting experiments on full scale vessels is extremely expensive and the budget is generally limited. Scaled models are good alternatives for cost reduction and convenient manipulation. Cole [1] systematically summarized the theoretical achievements and test phenomena related to UNDEX, and the empirical formulas to predict the shock wave loading and dynamic responses of the structures were also simplified. Brett et al. [2] investigated the dynamic responses of the steel cylinders exposed to near-field explosion by measuring the acceleration and underwater pressure. Li et al. [3] compared the linear and nonlinear responses and damage modes of the unfilled and main hull sand-filled cylindrical shell models subjected to underwater spherical explosion by a series of small-scale experiments. Chen et al. [4] experimentally investigated the strain and acceleration responses of a neoprene coated cylinder subjected to UNDEX in an artificial lake.

Developing an analytical solution to the UNDEX problem is extremely difficult because the dynamic responses of the vessels depend on many factors, including the complex structures, the detonation of the explosive charge, the propagation of the shock wave, the local cavitation, and the complicated fluid-structure interaction (FSI). Therefore, the theoretical studies are only suitable for simple geometrical structures. Huang [5, 6] employed the series expansion method and Laplace transform to elucidate the transient FSI of plane acoustic waves with submerged spherical and cylindrical elastic shells. Geers [7, 8] obtained the responses of the submerged cylindrical shell exited by a transient plane wave by using the residual potential method. Zhang and Geers [9] presented the transient response histories of the submerged

fluid-filled spherical shell exposed to a plane step wave. The separation of variables method was adopted and the results were compared with that of an empty submerged steel shell.

Over the last decades, with the improvement of computer technique and calculation procedure, a variety of numerical methods have been rapidly developed to analyze the FSI problem. The development of the finite element method (FEM) and boundary element method (BEM) makes it possible to investigate the responses of submerged complex structures subjected to noncontact UNDEX, and the small-scale model tests are frequently carried out to validate the feasibility of the numerical methods. Kwon and Fox [10] studied the nonlinear dynamic response of a cylinder subjected to a side-on, far-field UNDEX by using both numerical and experimental techniques. Wardlaw and Luton [11] presented several close-in cases to document the FSI mechanisms for internal and external UNDEX, and the rigid and deformable body simulations were compared by applying the coupled GEMINI–DYNA_N code. Mair [12] indicated that only codes employing "structural elements" were realistically applicable to the analysis of thin-walled structural response to UNDEX after reviewing the applicability of various hydrocode methodologies. Hung et al. [13] analyzed the linear and nonlinear dynamic responses of three cylindrical shell structures (unstiffened, internal, and external stiffened) subjected to small charge UNDEX in a water tank, and the dynamic accelerations and strains were compared with those obtained by FEM. Jin and Ding [14] compared the dynamic acceleration and velocity responses of a ship section between the experimental and numerical results by using ABAQUS.

Among the numerical techniques developed for the FSI problem, particularly worth mentioning is the doubly asymptotic approximation (DAA) method. Geers [15, 16] applied approximations approach in the limit of low and high frequency motions by using the virtual mass and plane wave approximation, and a smooth transition was effected in the intermediate frequency range to analyze the dynamic responses of the submerged structures subjected to UNDEX. Geers and Felippa [17] also studied the accuracy of the DAA forms through the numerical results of a submerged spherical shell. Liang and Tai [18] presented time history of the shock wave and the dynamic responses of a patrol boat subjected to underwater shock loading by using the FEM coupled with DAA. Lai [19] applied the time domain FEM/DAA coupling procedure to predict the transient dynamic responses of a submerged sphere shell with an opening subjected to UNDEX, and the results in the sea and air were also compared.

Most of the previous research mainly focused on the deformation, damage, and buckling of the cylindrical shells subjected to the shock wave. However, it is difficult to analyze the scattered wave of structures by the fluid-structure interaction method, and there are few studies on the incident wave in analytical method. Therefore, the research on the scattered wave field of submerged structures by the analytical methods seems to be very imperative. When the characteristic dimensions of small-sized submerged structures, such as towed vehicles and torpedoes, are much smaller than the wavelength, the scattering effect should be taken into consideration. In this paper, the coupled mode method is applied to decompose the incident wave into a series of harmonic waves. The scattering effect of submerged cylindrical shells is analyzed to verify that the conventional shock factor is excessively severe for small-sized structures. Therefore, the conventional shock factor is revised according to the impulse received by the cylindrical shell, which takes in the scattering effect of the characteristic dimensions of submerged structures. A set of numerical simulations are carried out by using the commercial code to validate the accuracy of the improved shock factor. Results show that the responses of cylindrical shells and spherical shells in different conditions are similar to each other when the improved shock factor is unchanged.

2. Shock Wave Pressure of UNDEX

UNDEX is the major threat to surface ships and submarines. According to the dynamic responses and damage modes of the vessels, the noncontact UNDEX can be divided into two kinds: near-field explosion and far-field explosion. In a near-field UNDEX, the structures are within the maximum radius $R_{\max}$ of the first pulsation of the gas bubble, and the shock energy of the explosive charge may cause great local damage to the vessels. For far-field UNDEX, the standoff distance R between the explosive charge and the structures is larger than the maximum radius $R_{\max}$, and the explosion can cause a wide range of nonrepair damage and failure of shipboard equipment. So the majority of the previous studies focus on the far-field explosion.

During an UNDEX, the sudden release of the explosive energy generates a transitory and highly compressed shock wave and a series of gas bubble pulsations. Most tests indicate that the damage and failure of the vessels occur at the early time of an UDNEX and are caused by the primary shock wave. The energy of the shock wave delivered to the vessels depends on the explosive charge weight and standoff distance. The shock wave is superimposed onto the hydrostatic pressure and propagates into the water medium in a spherical shape. The time history of the shock wave at a fixed location starts with an instantaneous peak pressure in time domain, followed by an exponentially decaying function. According to the empirical formula summarized by Cole [1] and Zamyshlyaev [20], the incident shock wave can be expressed by

$$p(t) = p_m e^{-(t-t_0)/\theta}, \tag{1}$$

where p_m denotes the peak magnitude of the pressure at the shock front; θ represents the time decay constant and t_0 is the propagation time from the explosive to the target. For trinitrotoluene (TNT), the peak pressure p_m and the time decay constant θ are

$$\begin{aligned} p_m &= K_1 \left(\frac{W^{1/3}}{R}\right)^{\alpha_1} \text{ Pa}, \\ \theta &= K_2 W^{1/3} \left(\frac{W^{1/3}}{R}\right)^{\alpha_2} \text{ ms}, \end{aligned} \tag{2}$$

where W is the explosive charge weight, R is the standoff distance, and K_1, K_2, α_1, and α_2 are the shock parameters of the explosive.

3. Coupled Mode Method

Cylindrical shells account for a large proportion of submerged structures. Many analytical approaches to the scattered wave field of cylindrical shells have been developed, such as the coupled mode method, the finite difference time domain method, and the reflected afterflow of virtual source method. In this paper, the coupled mode method is introduced to compute the scattered wave field by three-dimensional cylindrical shells for reducing computation time and ensuring precision.

A variety of researches on scattered wave field of harmonic wave have been conducted [21], but the incident wave induced by UNDEX is not a harmonic wave. It is necessary to decompose the incident wave into a series of harmonic plane waves with various frequencies. The incident wave can be expressed as

$$p_i(t) = p_m e^{-(t-t_0)/\theta}. \tag{3}$$

Assume $v = t - t_0$; then (3) is transformed into

$$p_i(v) = p_m e^{-v/\theta}, \quad v > 0. \tag{4}$$

The Fourier transform of (4) can be obtained:

$$p_i(\omega) = \int_{-\infty}^{\infty} p_i(v) e^{-j\omega v} dv. \tag{5}$$

The inverse Fourier transform of $p_i(\omega)$ is yielded as

$$p_i(v) = \frac{1}{2\pi} \int_{-\infty}^{\infty} p_i(\omega) e^{j\omega v} d\omega. \tag{6}$$

The incident wave can be regarded as plane wave, as the standoff distance is usually very large for the small-sized submerged structures. Hence, substituting (4) into (5) yields

$$p_i(\omega) = \frac{p_m}{1/\theta + j\omega}. \tag{7}$$

Substituting (7) into (6) yields

$$p_i(v) = \int_{-\infty}^{\infty} \frac{p_m}{2\pi\sqrt{\omega^2 + 1/\theta^2}} e^{j(\omega v - \gamma_0)} d\omega, \tag{8}$$

where $\gamma_0 = \omega\theta$.

The schematic diagram of scattered wave field of submerged cylindrical shell is shown in Figure 1, the explosive charge is located at point A, and the incident wave propagates along the y-axis direction. For conveniently computing the scattered wave field of cylindrical shell, the Cartesian coordinates (x, y, z) are transformed into cylindrical coordinates (r, ϕ, z).

Given that $OA = y_0$, c is the velocity of sound in water:

$$v = t - t_0 = t - \frac{r\cos\phi + y_0}{c}. \tag{9}$$

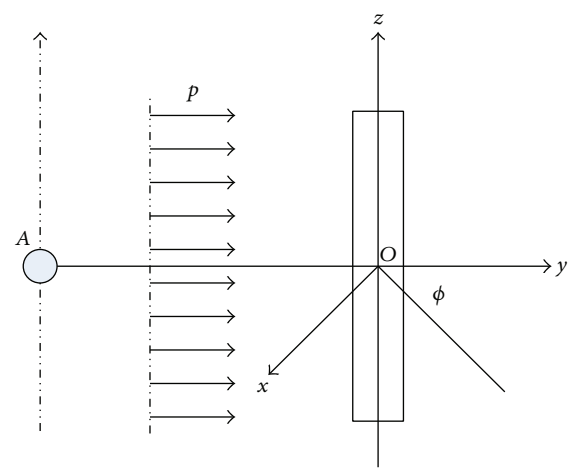

Figure 1: Scattered wave field of cylindrical shell.

In cylindrical coordinates, $p_i(v)$ can be written as $p_i(r, \phi, t)$ in the following expression:

$$p_i(r, \phi, t) = \frac{1}{2\pi} \int_{-\infty}^{\infty} p_i(r, \phi, \omega) d\omega, \tag{10}$$

where

$$p_i(r, \phi, \omega) = \frac{p_m}{\sqrt{\omega^2 + 1/\theta^2}} e^{j[\omega(t-(r\cos\phi + y_0)/c) - \gamma_0]}. \tag{11}$$

Let

$$\begin{aligned} P_0 &= \frac{p_m}{2\pi\sqrt{\omega^2 + 1/\theta^2}}, \\ p_i(r, \phi) &= P_0 e^{-jkr\cos\phi}, \\ \gamma_1 &= k y_0 + \gamma_0, \end{aligned} \tag{12}$$

where $k = \omega/c$ is the wave number; then (11) can be written as

$$p_i(r, \phi, \omega) = p_i(r, \phi) e^{j(\omega t - \gamma_1)}. \tag{13}$$

We can see that $p_i(r, \phi, \omega)$ is a harmonic plane wave, and the incident wave is decomposed into the integral of harmonic plane wave. The scattered wave field of submerged cylindrical shells can be obtained by (10) and (13).

For a homogeneous cylindrical shell in infinite flow field, as shown in Figure 1, its outer radius and inner radius are a and b, respectively. The scalar and vector potential functions are Φ and Π, respectively. Boundary conditions of the fluid-structure interface should satisfy the following equations:

$$u_r = \frac{1}{\omega^2 \rho} \frac{\partial p}{\partial r};$$

$$\sigma_{rr} = -p;$$

$$\begin{aligned} &\sigma_{r\phi} = 0, \\ &\qquad\qquad\qquad\qquad r = a, \\ &\sigma_{rr} = 0; \\ &\sigma_{r\phi} = 0, \\ &\qquad\qquad\qquad\qquad r = b, \end{aligned} \tag{14}$$

where u and σ are displacement and stress, respectively. ρ is the density of the fluid, and p is the total sound pressure of harmonic wave components and can be written as

$$p = p_i(r, \phi, \omega) + p_s(r, \phi, \omega), \tag{15}$$

where $p_s(r, \phi, \omega)$ is the sound pressure of the scattered wave induced by harmonic wave components.

The sound field can be decomposed in cylindrical functions:

$$\begin{aligned} &p_i(r, \phi, \omega) \\ &\quad = \frac{p_m}{\sqrt{\omega^2 + 1/\theta^2}} e^{j(\omega t - \gamma_1)} \sum_{n=0}^{\infty} \varepsilon_n j^n J_n(kr) \cos n\phi, \\ &p_s(r, \phi, \omega) \\ &\quad = \frac{p_m}{\sqrt{\omega^2 + 1/\theta^2}} e^{j(\omega t - \gamma_1)} \sum_{n=0}^{\infty} A_n H_n^{(2)}(kr) \cos n\phi. \end{aligned} \tag{16}$$

The potential functions can be decomposed as

$$\begin{aligned} \Phi &= \frac{p_m}{\sqrt{\omega^2 + 1/\theta^2}} \\ &\quad \cdot e^{j(\omega t - \gamma_1)} \sum_{n=0}^{\infty} \left[B_n J_n(k_l r) + C_n N_n(k_l r)\right] \cos n\phi, \\ \Pi &= \frac{p_m}{\sqrt{\omega^2 + 1/\theta^2}} \\ &\quad \cdot e^{j(\omega t - \gamma_1)} \sum_{n=1}^{\infty} \left[D_n J_n(k_t r) + E_n N_n(k_t r)\right] \sin n\phi, \end{aligned} \tag{17}$$

where $\varepsilon_n = 1$ for $n = 0$ and $\varepsilon_n = 2$ for $n > 0$. J_n and N_n are, respectively, Bessel function and Neumann function of order n. $H_n^{(2)}$ is Hankel function of the second kind of order n. Substituting (16) and (17) into geometric equation, constructive equation, and wave equation [22], a group of functions of undetermined coefficients can be obtained as

$$MP = U, \tag{18}$$

where coefficient matrix M is a square matrix of order 5 and U and P are column vectors of order 5. Undetermined coefficients $P = [A_n, B_n, C_n, D_n, E_n]^T$ can be obtained by solving the linear equation. Thus the scattered wave field can be expressed by the harmonic waves. The pressure distribution on the surface of cylindrical shell is given by

$$\begin{aligned} p(a, \phi, \omega) &= \frac{p_m}{\sqrt{\omega^2 + 1/\theta^2}} \\ &\quad \cdot e^{j(\omega t - \gamma_1)} \sum_{n=0}^{\infty} \left[\varepsilon_n j^n J_n(ka) + A_n H_n^{(2)}(ka)\right] \cos n\phi. \end{aligned} \tag{19}$$

4. Shock Factor Revision

Shock factor is defined to describe the shock environment for surface ships and submerged vessels subjected to UNDEX. The responses of structures which suffered from UNDEX should be approximately similar to each other when the shock factor is unchanged. The widely used shock factor is

$$C = \frac{\sqrt{W}}{R}. \tag{20}$$

It is defined in terms of equal shock energy sheltered by structures based on the hypothesis of plane wave. The total energy of incident wave is

$$E_t = W \rho_e \eta_e, \tag{21}$$

where ρ_e is the chemical energy of explosive charge of unit mass and η_e is the conversion rate from chemical energy to incident wave energy. If the standoff distance is large enough compared with the characteristic dimensions of the structures, the incident wave can be regarded as plane wave. The energy sheltered by the structures is

$$E_s = E_t \frac{S_e}{4\pi R^2}, \tag{22}$$

where S_e is the projected area of structures in the vertical incident wave front. Thus the relationship between C and E_s can be obtained as

$$E_s = \frac{\rho_e \eta_e S_e C}{4\pi}. \tag{23}$$

Generally, S_e is constant. So the sheltered energy E_s is also constant when the shock factor C remains unchanged.

The conventional shock factor C is suitable to assess the shock environment of surface ships and submarines. When the characteristic dimension of submerged structures is much smaller than the wavelength of incident wave induced by UNDEX, the scattered effect of submerged structures should be taken into consideration. In this paper, a set of cylindrical shells with different diameters are applied to investigate how characteristic dimension affects the scattered wave field.

The schematic diagram of the cylindrical shells with different diameters that suffered from an UNDEX is shown in Figure 3. For eliminating the effect of water surface, the cylindrical shells are set 50 m underwater, and the cylindrical shells and explosive charge are placed at the same depth. The shells are produced by using the stainless steel whose strain-stress curve is depicted in Figure 2. The material properties and the parameters of UNDEX are given in Table 1.

Table 1: Material properties and parameters of UNDEX.

Parameters	
Young's modulus (GPa)	210
Poisson's ratio	0.3
Mass density (km/m^3)	7850
Mass of explosive charge (kg)	1000
Standoff distance (m)	100
Length of shells (m)	20

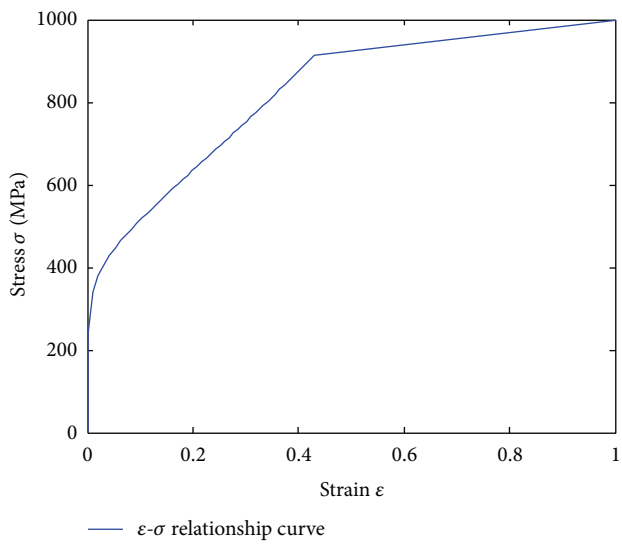

Figure 2: Strain-stress curve of stainless steel.

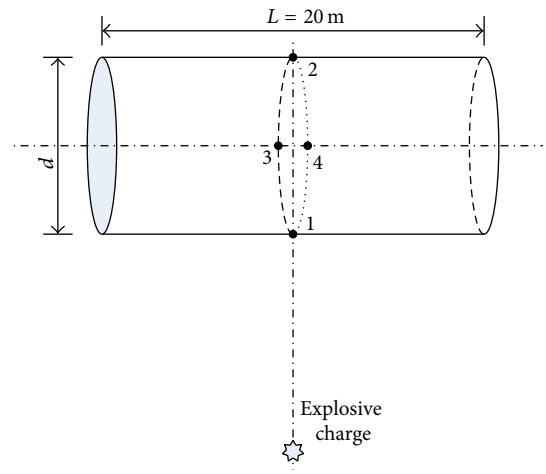

Figure 3: Top view of cylindrical shell.

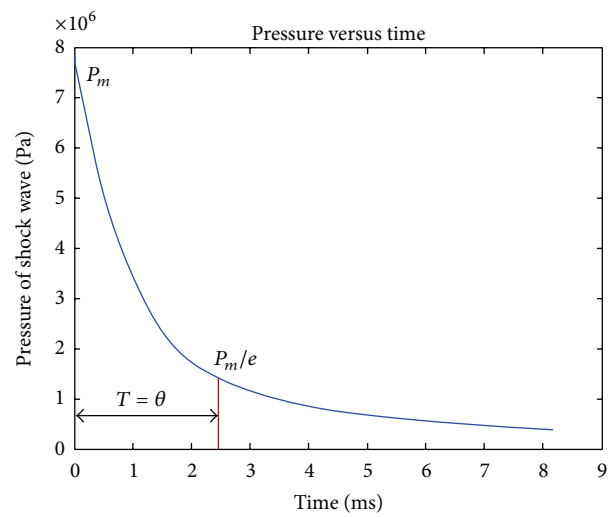

Figure 4: Incident wave with pulse width.

The incident wave can be decomposed into a series of harmonic waves, and the pressure distribution on the surface of cylindrical shells can be calculated by the coupled mode method. So the time history of average pressure of center point 1 on the front surface of the shell can be obtained. Cole extensively discussed the important meaning of impulse and energy flux density, which can be used to estimate the initial velocity of structures subjected to UNDEX. Then the impulse of point 1 in shock wave period is calculated to evaluate the influence of the diameters of cylindrical shells on the scattered wave field. The impulse can be expressed as

$$I = \int_0^{6.7\theta} p(t)\,dt. \tag{24}$$

It is well known that the frequency of the incident wave makes a great influence on the meshing size of fluid element in the fluid-structure interaction. The maximum frequency of the incident wave can be defined as the reciprocal of pulse width [23]. As shown in Figure 4, the constant θ represents the time duration from p_m to p_m/e. Thus the constant θ is defined as the pulse width of the incident wave and the wavelength can be calculated by $\lambda = c\theta$.

The impulses of point 1 on the cylindrical shells with different diameter are calculated, and the results are listed in Table 2. In the case analysis, the diameters range from 0.1 m to 5 m, but the standoff distance remains constant. It is obviously observed that the impulse significantly decreases as the diameters reduce. This illustrates that the scatter effect should be taken into consideration when the diameters of cylindrical shells are much smaller than the wavelength of the incident wave. Figure 5 shows the relationship between the impulses and the ratio $\eta = d/\lambda$ by taking a nonlinear regression. The regressive curve is expressed as

$$I = 2377e^{-0.19\lambda/d} + 5269. \tag{25}$$

In Figure 5, the impulse approximately begins to decrease when $d/\lambda < 2$ and rapidly decays in an exponential function when $d/\lambda < 1$. It means that the collection pressure of the cylindrical shells decreases. This can be explained by the fact that part of the shock energy diffracts when the diameters of the cylindrical shells are relatively smaller than the wavelength. Thus the conventional shock factor is too severe for the small-sized submerged structures. In order

Table 2: Calculated impulses of cylindrical shells with different diameters.

Cases	Diameter (m)	d/λ	Impulse (N∗m)
1	0.1	0.07	5423
2	0.2	0.13	5859
3	0.3	0.2	6198
4	0.4	0.27	6375
5	0.5	0.34	6517
6	0.6	0.4	6705
7	0.7	0.47	6882
8	0.8	0.54	6997
9	0.9	0.61	7088
10	1	0.67	7193
11	1.5	1.01	7295
12	2	1.35	7323
13	2.5	1.69	7384
14	3	2.04	7412
15	4	2.7	7439
16	5	3.33	7451

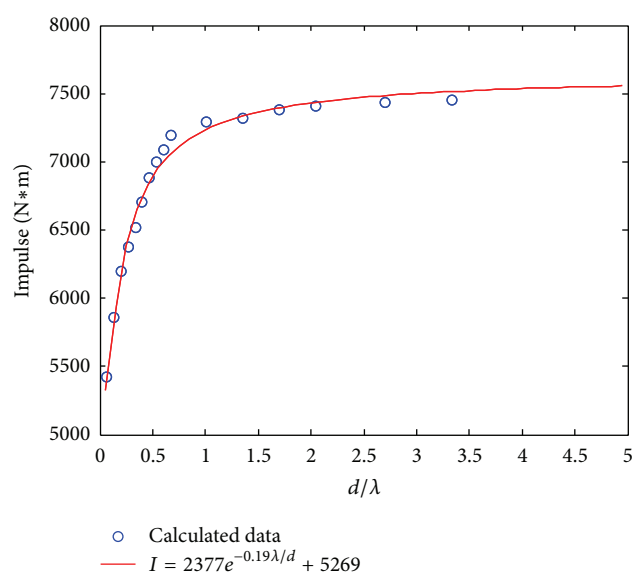

Figure 5: Schematic diagram of regression curve.

to revise the scattering effect, an improved shock factor is defined as

$$C_m = Ce^{-0.19\lambda/d} = \frac{\sqrt{W}}{R} e^{-0.0233\sqrt[3]{W}(\sqrt[3]{W}/R)^{-0.23}/d}, \quad (26)$$

where d is the characteristic dimension of submerged structures. The relationship between the improved shock factor and conventional shock factor is depicted in Figure 6. It is observed that the improved shock factor clearly differs from the conventional one just when the characteristic dimension is relatively smaller than the wavelength. There is almost no difference between them when the characteristic dimension is much larger than the wavelength.

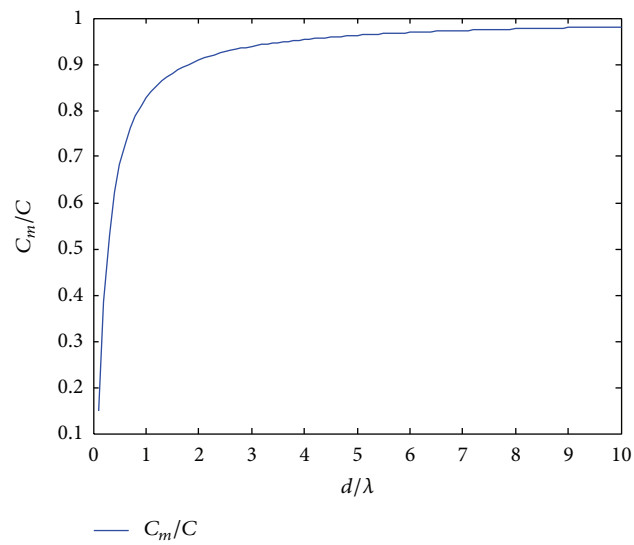

Figure 6: The relationship between the improved and conventional shock factors.

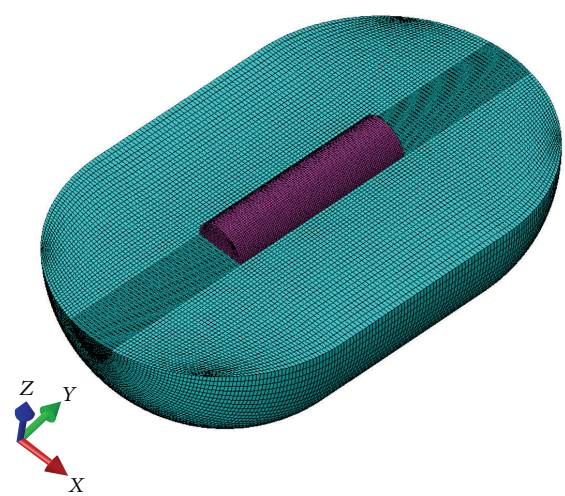

Figure 7: The finite element model of the cylindrical shell and water.

5. Numerical Simulations

In the past decades, numerical methods have been developed rapidly and applied successfully to analyze the responses of submerged structures under shock loading. To verify the accuracy of the coupled mode method, some conditions in Table 2 are simulated by commercial code. As shown in Figure 7, the cylindrical shell and the outer fluid field are modeled by using the shell element and acoustics element, respectively, and an impedance-type radiation boundary condition is applied at the outer surface of the fluid mesh.

The time histories of acoustic pressure at point 1 on the front surface of the cylindrical shells are illustrated in Figure 8 to compare with that calculated by using the coupled mode method. It is observed that both the peak values and the attenuation trend are in good accordance with each other. Meanwhile, there is a disability for the coupled mode method

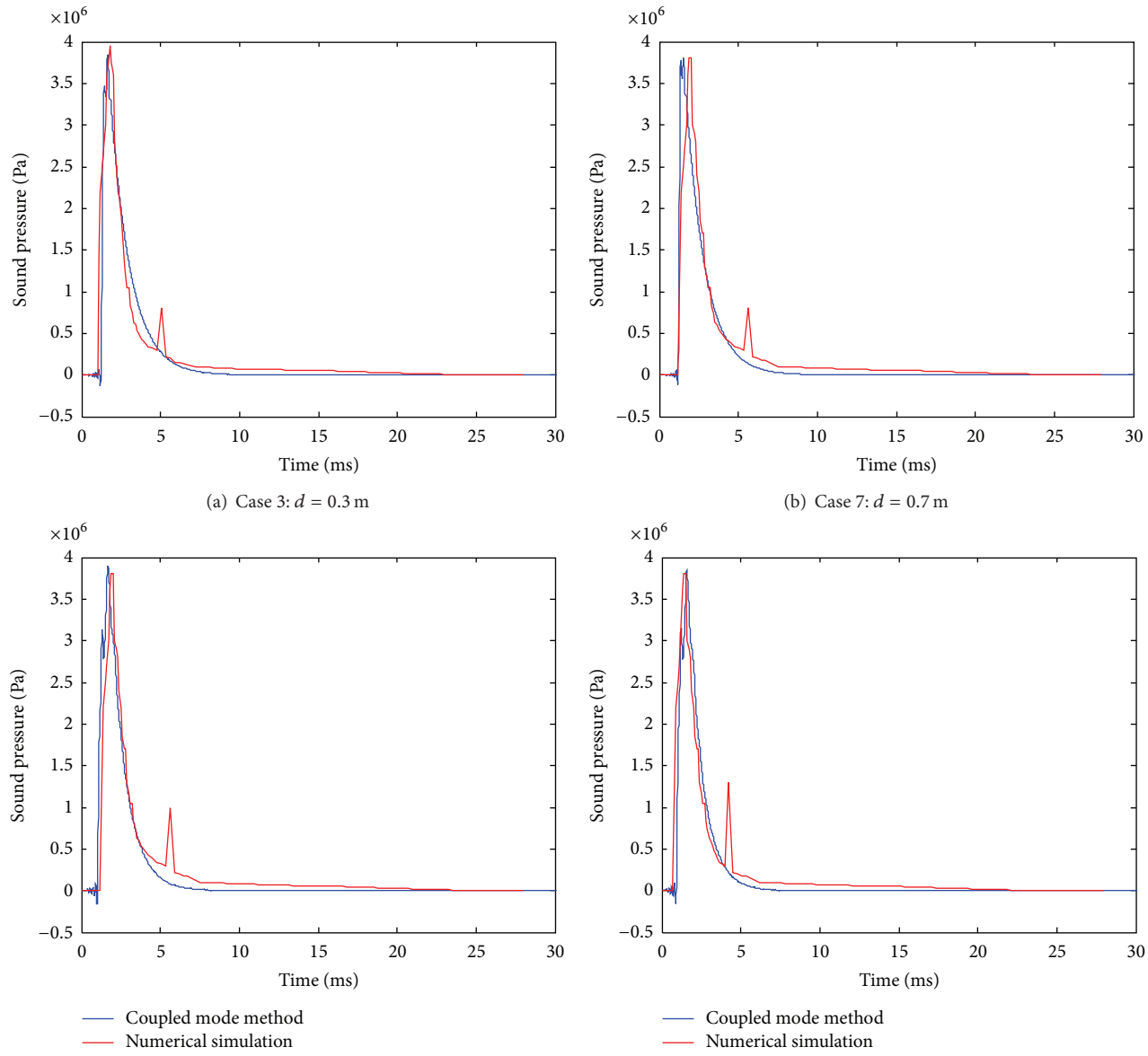

(a) Case 3: $d = 0.3$ m

(b) Case 7: $d = 0.7$ m

(c) Case 10: $d = 1.0$ m

(d) Case 14: $d = 3.0$ m

Figure 8: Comparison of the time history of sound pressure.

to calculate the reflection sound pressure from the cylindrical shells. The reflection sound pressure can be omitted due to small amplitude and short time. Therefore, the coupled mode method is possessed of high accuracy to calculate the sound field of submerged cylindrical shells.

To verify the accuracy and effectiveness of the revised shock factor, the responses of cylindrical shells and spherical shells are studied by numerical simulations. A set of different cases with different shock factors are carried out by the commercial code ABAQUS. The mass of explosive charge varies from 100 kg to 1000 kg, and the standoff distance varies from 25 m to 60 m. The revised shock factor remains unchanged in Tables 3 and 4. For efficient solution, the diameter and length of the cylindrical shell are set to 0.6 m and 2 m, respectively. The diameter and the thickness of the spherical shell are set to 0.6 m and 0.008 m, respectively.

Table 3: Acceleration peak values of cylindrical shells in different cases.

Cases	Explosive charge (kg)	Standoff (m)	C_m	C	Peak value (m/s^2)
1	100	37		0.27	52551
2	200	48	0.20	0.29	52700
3	350	60		0.31	53025
4	200	26		0.54	76979
5	350	32	0.40	0.58	75187
6	500	36		0.62	76184
7	500	25		0.89	102513
8	750	29	0.60	0.94	102078
9	1000	32		0.98	103608

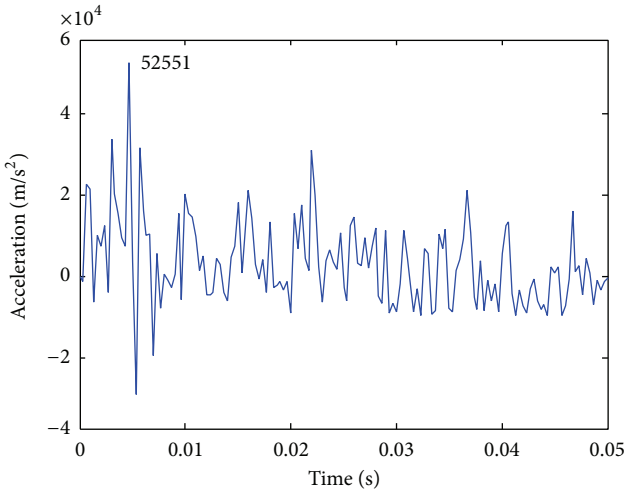

$W = 100$ kg, $R = 37$ m

(a) Case 1: $C_m = 0.20$, $C = 0.27$

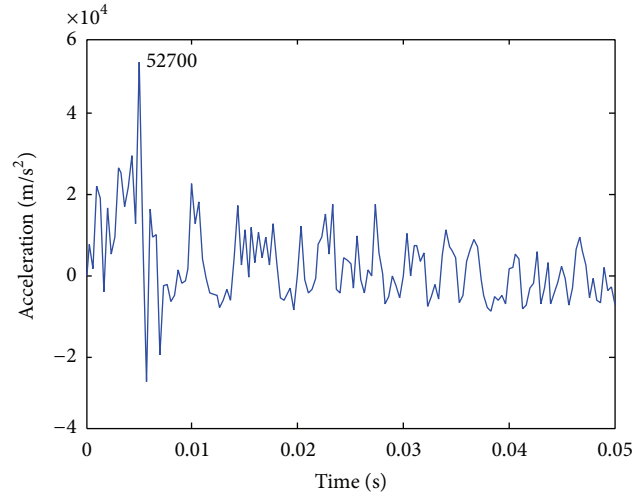

$W = 200$ kg, $R = 48$ m

(b) Case 2: $C_m = 0.20$, $C = 0.29$

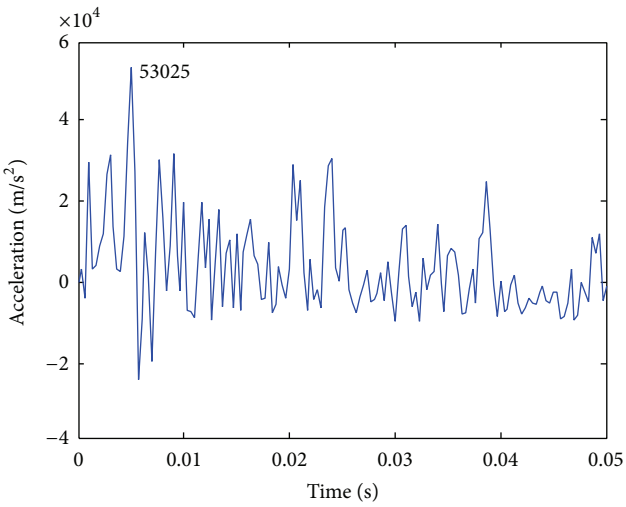

$W = 350$ kg, $R = 60$ m

(c) Case 3: $C_m = 0.20$, $C = 0.31$

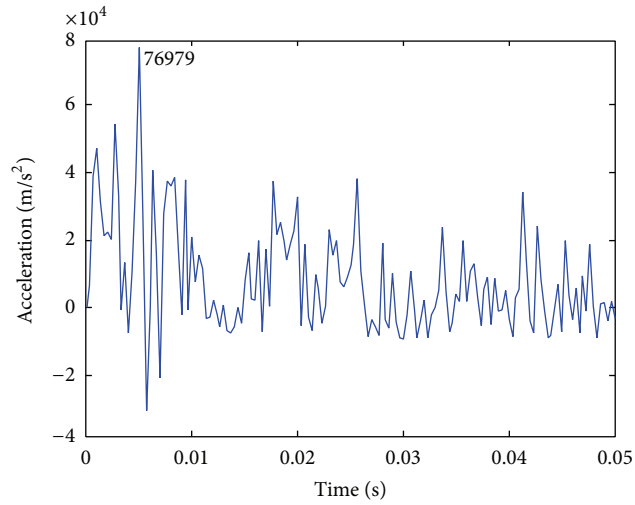

$W = 200$ kg, $R = 26$ m

(d) Case 4: $C_m = 0.40$, $C = 0.54$

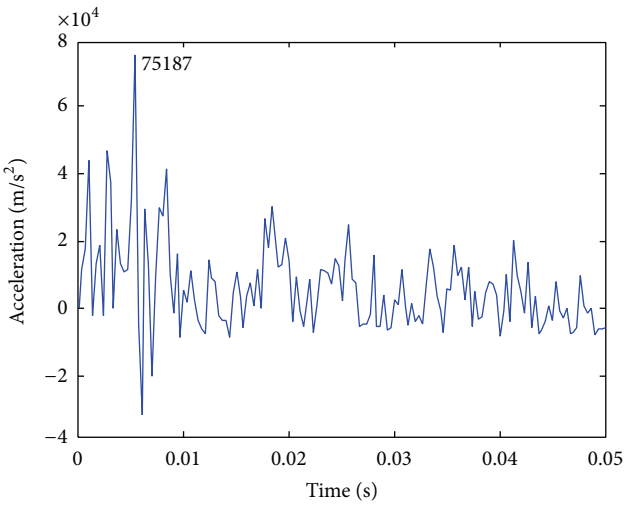

$W = 350$ kg, $R = 32$ m

(e) Case 5: $C_m = 0.40$, $C = 0.58$

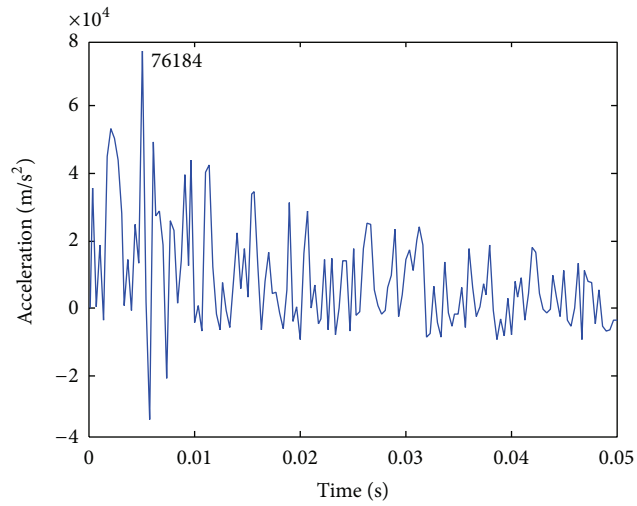

$W = 500$ kg, $R = 36$ m

(f) Case 6: $C_m = 0.40$, $C = 0.62$

Figure 9: Continued.

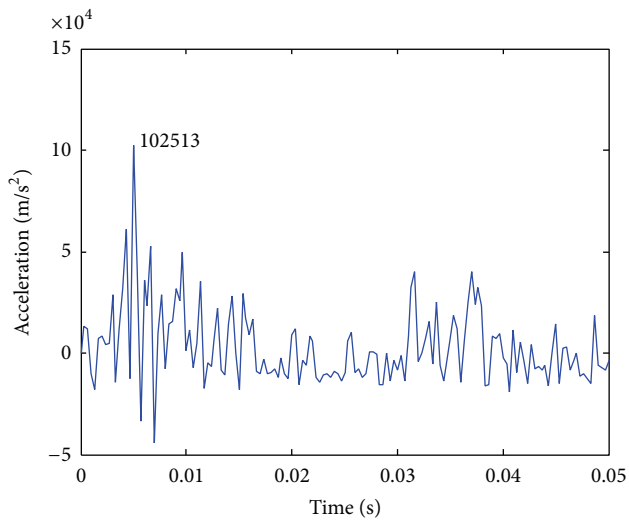

(g) Case 7: $C_m = 0.60$, $C = 0.89$

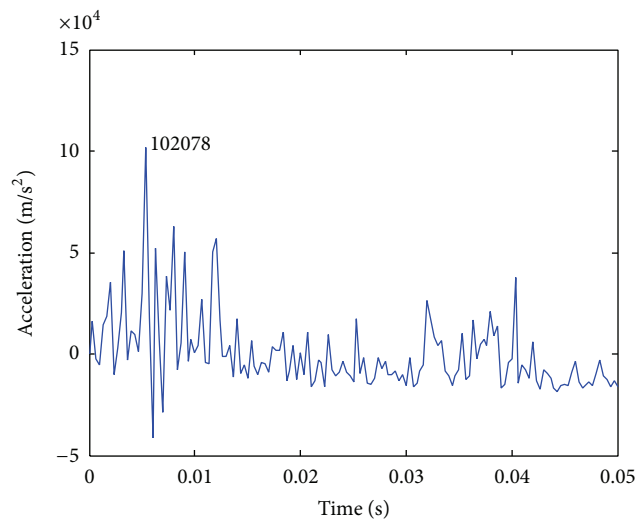

(h) Case 8: $C_m = 0.60$, $C = 0.94$

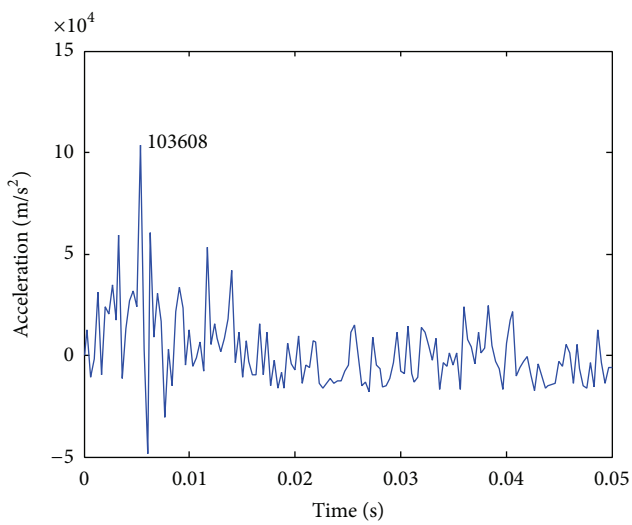

(i) Case 9: $C_m = 0.60$, $C = 0.98$

Figure 9: The time history of dynamic acceleration of cylindrical shells.

Table 4: Acceleration peak values of spherical shells in different cases.

Cases	Explosive charge (kg)	Standoff (m)	C_m	C	Peak value (m/s^2)
10	100	37		0.27	51963
11	200	48	0.20	0.29	51495
12	350	60		0.31	51024

The large acceleration is the major reason for the damage of the instruments in surface ships and submarines subjected to UNDEX. Therefore, the acceleration responses of cylindrical shells and spherical shells are calculated. The time histories of acceleration of the central point on the front surface of the cylindrical shells are depicted in Figure 9, and the acceleration peak values are listed in Table 3. The peak values hardly vary when the improved shock factor is the same value, and the maximum error of acceleration peak value is approximately 0.90%, 2.38%, and 1.50% when the improved shock factor is 0.20, 0.40, and 0.60, respectively. This means that the acceleration responses of cylindrical shells are about the same when the improved shock factor is unchanged.

The finite element model of the spherical shell is depicted in Figure 10, and the time histories of acceleration of the central point on the front surface are also depicted in Figure 10. The acceleration peak values are listed in Table 4.

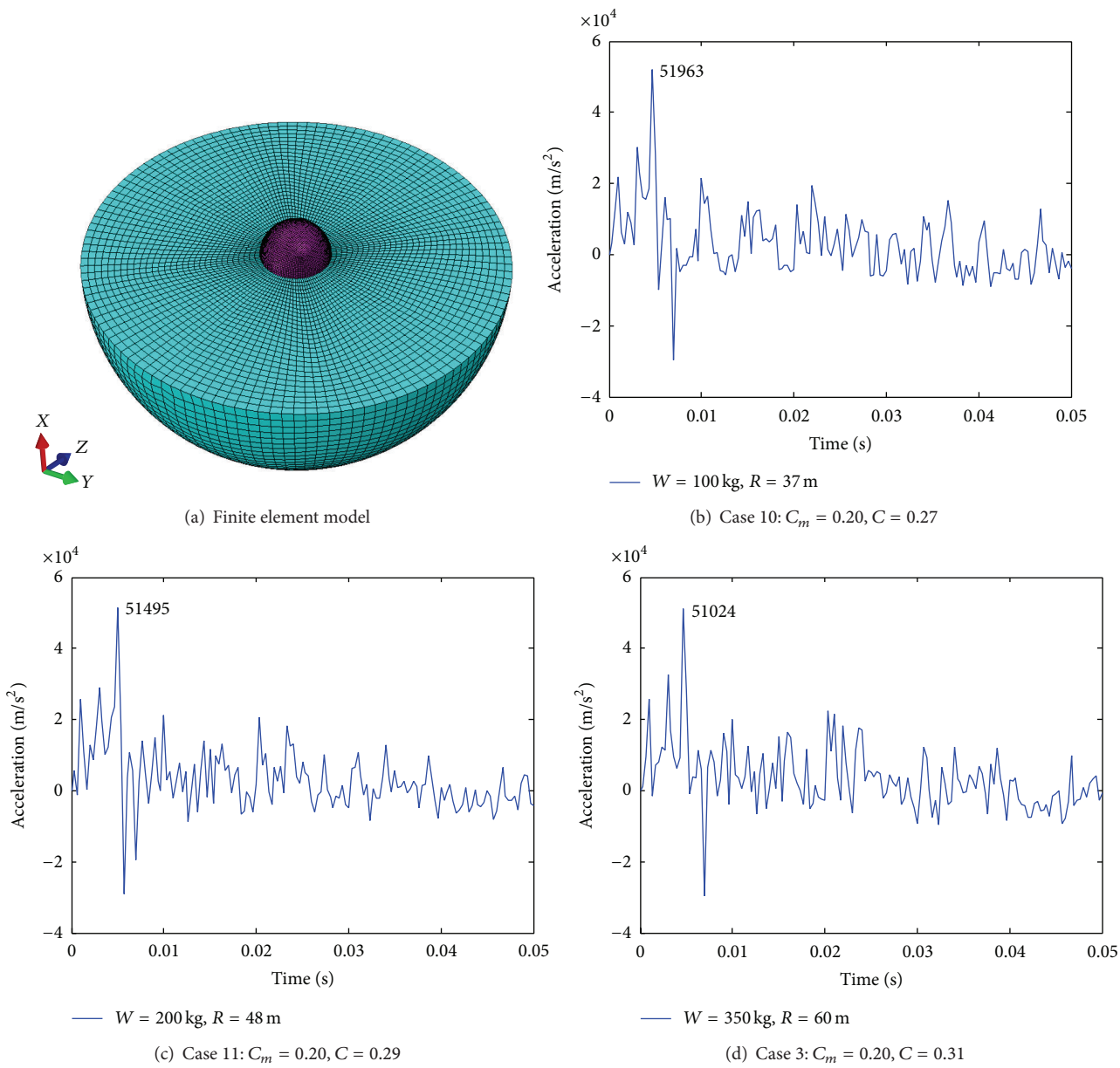

(a) Finite element model

(b) Case 10: $C_m = 0.20$, $C = 0.27$

(c) Case 11: $C_m = 0.20$, $C = 0.29$

(d) Case 3: $C_m = 0.20$, $C = 0.31$

Figure 10: The finite element model and time history of dynamic acceleration of spherical shells.

The maximum error of acceleration peak value is approximately 1.84% when the improved shock factor is 0.20. The acceleration responses of spherical shells hardly vary when the improved shock factor remains unchanged.

6. Conclusions

The conventional shock factor is aimed at large surface ships and submarines, in which the effect from scattering is ignored. When the characteristic dimension of submerged structures is relatively smaller than the wavelength of the incident wave, the scattering can greatly affect the impact load.

In this study, the incident wave is decomposed into a series of harmonic waves, and the scatter wave field of submerged cylindrical shells is calculated by using the coupled mode method. A regression equation is developed between the impulses and ratio of the diameters of the shells and the wavelength of the incident wave. An improved shock factor is achieved based on the fitted curve, which consists of the scattering effect caused by the diameters of the submerged cylindrical shells. The improved shock factor clearly differs from the conventional one when the characteristic dimension is relatively smaller than the wavelength, and the results of two shock factors are getting more and more closer with the increase of characteristic dimension.

The acceleration responses of shells in different conditions are calculated too. Results show that the shock responses of cylindrical shells and spherical shells are about the same when the improved shock factor is unchanged.

Conflict of Interests

The authors declare that there is no conflict of interests regarding the publication of this paper.

References

[1] R. H. Cole, *Underwater Explosions*, Princeton University Press, Princeton, NJ, USA, 1948.

[2] J. M. Brett, G. Yiannakopoulos, and P. J. van der Schaaf, "Time-resolved measurement of the deformation of submerged cylinders subjected to loading from a nearby explosion," *International Journal of Impact Engineering*, vol. 24, no. 9, pp. 875–890, 2000.

[3] L. J. Li, W. K. Jiang, and Y. H. Ai, "Experimental study on deformation and shock damage of cylindrical shell structures subjected to underwater explosion," *Proceedings of the Institution of Mechanical Engineers, Part C: Journal of Mechanical Engineering Science*, vol. 224, pp. 2505–2514, 2010.

[4] Y. Chen, Y. Wang, Z. Y. Zhang, and H. X. Hua, "Experimental research on the responses of neoprene coated cylinder subjected to underwater explosions," *Journal of Offshore Mechanics and Arctic Engineering-Transactions of the Asme*, vol. 135, no. 1, Article ID 011102, 2013.

[5] H. Huang, "Transient interaction of plane acoustic waves with a spherical elastic shell," *Journal of the Acoustical Society of America*, vol. 45, no. 3, pp. 661–670, 1969.

[6] H. Huang, "An exact analysis of the transient interaction of acoustic plane waves with a cylindrical elastic shell," *Journal of Applied Mechanics*, vol. 37, no. 4, pp. 1091–1099, 1970.

[7] T. L. Geers, "Excitation of an elastic cylindrical shell by a transient acoustic wave," *Journal of Applied Mechanics*, vol. 36, pp. 459–469, 1969.

[8] T. L. Geers, "Response of an elastic cylindrical shell to a transverse acoustic shock wave in a light fluid medium," *Journal of the Acoustical Society of America*, vol. 48, no. 3, pp. 692–701, 1970.

[9] P. Z. Zhang and T. L. Geers, "Excitation of a fluid—filled, submerged spherical shell by a transient acoustic wave," *Journal of the Acoustical Society of America*, vol. 93, pp. 696–705, 1993.

[10] Y. W. Kwon and P. K. Fox, "Underwater shock response of a cylinder subjected to a side-on explosion," *Computers & Structures*, vol. 48, no. 4, pp. 637–646, 1993.

[11] A. B. Wardlaw Jr. and J. A. Luton, "Fluid-structure interaction mechanisms for close-in explosions," *Shock and Vibration*, vol. 7, no. 5, pp. 265–275, 2000.

[12] H. U. Mair, "Review: hydrocodes for structural response to underwater explosions," *Shock and Vibration*, vol. 6, no. 2, pp. 81–96, 1999.

[13] C. F. Hung, B. J. Lin, J. J. Hwang-Fuu, and P. Y. Hsu, "Dynamic response of cylindrical shell structures subjected to underwater explosion," *Ocean Engineering*, vol. 36, no. 8, pp. 564–577, 2009.

[14] Q. K. Jin and G. Y. Ding, "A finite element analysis of ship sections subjected to underwater explosion," *International Journal of Impact Engineering*, vol. 38, no. 7, pp. 558–566, 2011.

[15] T. L. Geers, "Residual potential and approximate methods for three-dimensional fluid-structure interaction problems," *The Journal of the Acoustical Society of America*, vol. 49, no. 5B, p. 1505, 1971.

[16] T. L. Geers, "Doubly asymptotic approximations for transient motions of submerged structures," *The Journal of the Acoustical Society of America*, vol. 64, no. 5, pp. 1500–1508, 1978.

[17] T. L. Geers and C. A. Felippa, "Doubly asymptotic approximations for vibration analysis of submerged structures," *Journal of the Acoustical Society of America*, vol. 73, pp. 1152–1159, 1983.

[18] C.-C. Liang and Y.-S. Tai, "Shock responses of a surface ship subjected to noncontact underwater explosions," *Ocean Engineering*, vol. 33, no. 5-6, pp. 748–772, 2006.

[19] W.-H. Lai, "Transient dynamic response of submerged sphere shell with an opening subjected to underwater explosion," *Ocean Engineering*, vol. 34, no. 5-6, pp. 653–664, 2007.

[20] B. V. Zamyshlyaev, "Dynamic loads in underwater explosion," Report AD-757183, 1973.

[21] J. A. Fawcett, "Coupled-mode modeling of acoustic scattering from three-dimensional, axisymmetric objects," *The Journal of the Acoustical Society of America*, vol. 102, no. 6, pp. 3387–3393, 1997.

[22] J. Lubliner, *Plasticity Theory*, Courier Dover Publications, Mineola, NY, USA, 2008.

[23] Z. H. Bai, *Model method of shock environment in ship far-field underwater explosion [M.S. thesis]*, Harbin Engineering University, Harbin, China, 2012.